Mechanism of activation of bacterial cellulose synthase by cyclic-di-GMP

Jacob L. W. Morgan[1], Joshua T. McNamara[1] and Jochen Zimmer[1]

[1]*Center for Membrane Biology*

Department of Molecular Physiology and Biological Physics

University of Virginia

Charlottesville, VA, USA

Correspondence to: Jochen_Zimmer@virginia.edu

Supplementary Information

Supplementary Figures 1 - 7

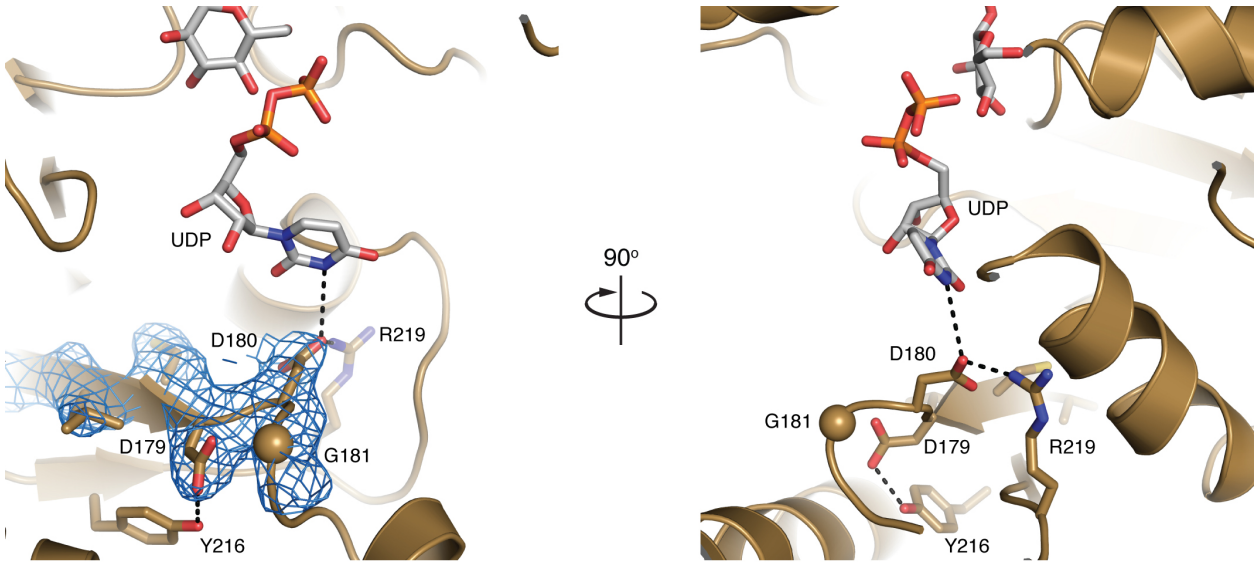

Supplementary Figure 1 Correction of a register shift in BcsA. A register shift in BcsA (residues 171 to 190) has been corrected in the new structure. The new 2.65 Å electron density map allows the unambiguous assignment of the register in this β-strand. The corrected register positions Asp179 of the conserved "DDG" motif in hydrogen bonding distance to the conserved Tyr216 and Asp180 in hydrogen bonding distance to the UDP uracil moiety and the conserved Arg219. A SigmaA-weighted 2mFo-DFc electron density contoured at 1 σ is shown as a blue mesh. UDP and the translocating glucan as observed in pdb 4HG6 are shown as gray sticks.

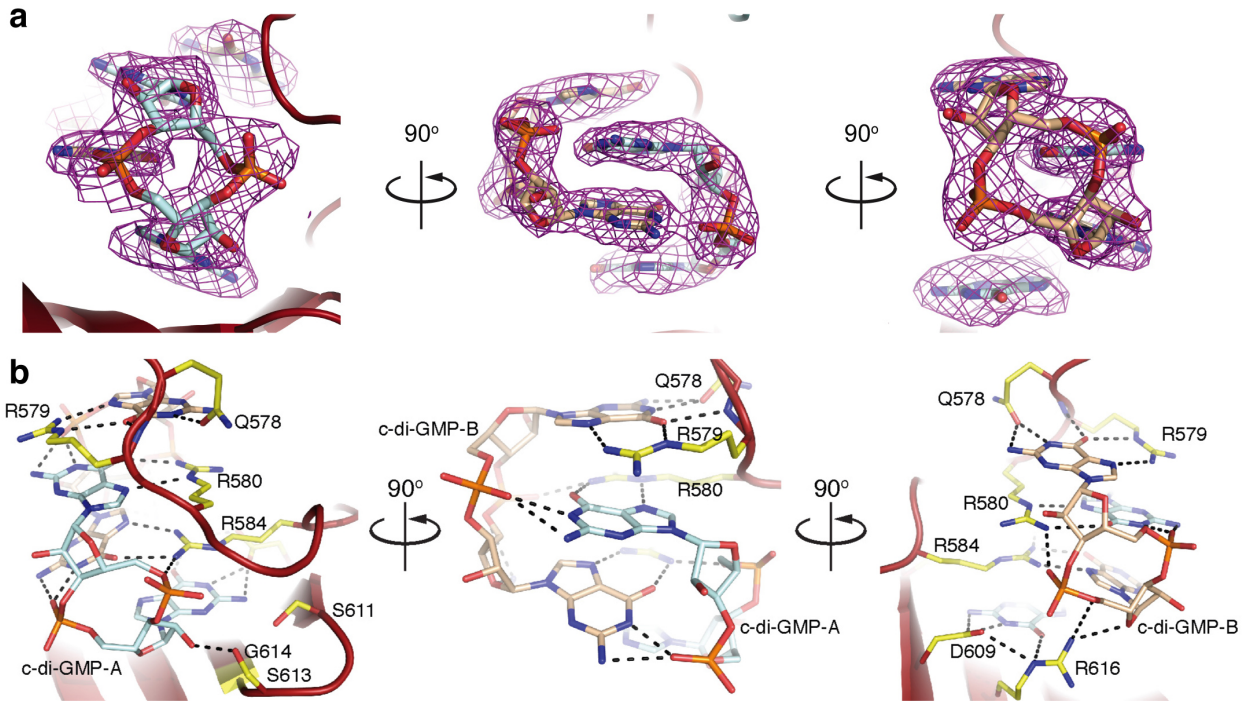

Supplementary Figure 2 Cyclic-di-GMP binding to BcsA. (**a**) An intercalated homodimer of c-di-GMP binds to BcsA's PilZ domain. An unbiased SigmaA-weighted mFo-DFc difference electron density for c-di-GMP contoured at 4σ is shown as a magenta mesh. The density was calculated after refining the protein structure and before placing any ligands. The c-di-GMP dimer is shown in sticks colored light blue or pale brown for the carbon atoms, respectively.

(**b**) BcsA's PilZ domain tightly coordinates a c-di-GMP dimer, c-di-GMP-A and –B. One guanylate group of c-di-GMP-A (GA1) packs its guanine group into a pocket on the β-barrel surface formed by the conserved Gly614 and Gly670 where it is further stabilized by side chain interactions with Asp609 of the "DxSxxG" motif as well as Ser613 and Arg616. The guanine interacts with Asp609 via its cyclic N1 atom and exocyclic amine group and its carbonyl oxygen contacts the guanidinium group of Arg616. Ser611 of the "DxSxxG" motif does not directly contact GA1, however, it is likely that its interaction is mediated by an unresolved water molecule. The 2' hydroxyl of the GA1 ribose interacts with the hydroxyl group of Ser613. Arg584 of the TM8-β-barrel linker stacks on top of the GA1 guanine and forms a salt bridge with the phosphate group belonging to the second guanylate of c-di-GMP-A (GA2). The side chain of the invariant Arg580 of the TM8-β-barrel linker is co-planar with the guanine of GA2 and forms hydrogen bonds via its guanidinium group with the GA2's guanine N7 and carbonyl oxygen. Similar to the stacking interactions observed for GA1, the preceding Arg579 stacks on top of the GA2 guanine group. The ring N1 and exocyclic amine group of GA2 interact with the phosphate moiety of the second c-di-GMP molecule (c-di-GMP-B).

C-di-GMP-B makes fewer interactions with BcsA and is primarily stabilized by c-di-GMP-A and residues belonging to the TM8-β-barrel linker. Its first guanylate closest to the β-barrel surface (GB1) forms π–π stacking interactions with the guanine of GA2 and hydrogen bonds via its ring N7 and carbonyl oxygen with Arg584, the same residue that stacks on top of the GA1 guanine. As observed for the guanine group of GA2, its ring N1 and exocyclic amine contact the phosphate group of the other c-di-GMP molecule, thereby stabilizing the intercalated c-di-GMP dimer. The second guanylate of c-di-GMP-B (GB2) interacts via its ring carbonyl oxygen with the backbone nitrogen as well as the Nε of the co-planar Arg579 and via the guanine's N1 and exocyclic amine with the invariant Gln578 of the TM8-β-barrel linker. In addition, its phosphate group forms a salt bridge with Arg580 that is co-planar with the guanine of GA2.

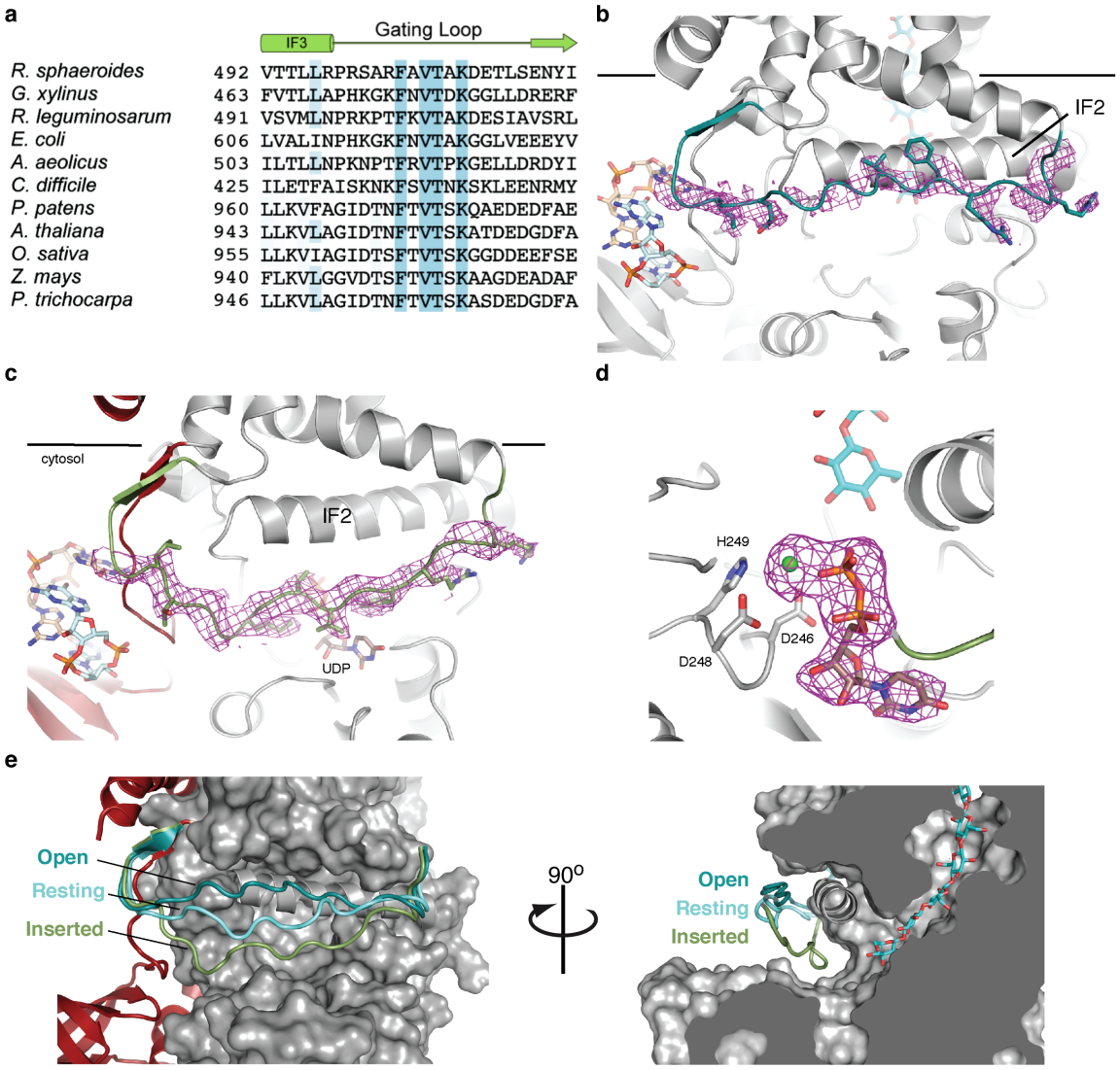

Supplementary Figure 3 Conformational changes of BcsA's gating loop. (**a**) Sequence conservation of the gating loop. The "FxVTxK" motif is conserved in pro- and eukaryotic cellulose synthases. (**b**) Unbiased SigmaA-weighted 2mFo-DFc electron density for the gating loop in the "up" position shown as a magenta mesh and contoured at 1σ. The density was calculated before modeling the gating loop. The position of the loop's backbone is well resolved (colored cyan). The side chains of Phe503 and Val505 pack into a hydrophobic pocket on IF2 and are well resolved in the original density map. (**c** and **d**) Unbiased SigmaA-weighted mFo-DFc difference electron density for the gating loop in the "down" position and UDP, shown as a magenta mesh. The density was calculated before modeling the gating loop and placing UDP/Mg and is contoured at 2.5σ and 3σ for the gating loop and UDP, respectively. The position of the entire gating loop backbone is well resolved and so are the side chains of the conserved Phe503, Val505, Thr506 and Lys508. Additional electron density between the UDP β-phosphate and BcsA's "DxD'" motif is consistent with a bound magnesium ion (shown as a green sphere). UDP is shown in sticks colored violet for the carbon atoms and the gating loop is colored green. (**e**) Front and side view comparing the three gating loop positions observed in the resting and c-di-GMP bound states. BcsA is shown as a gray surface with the PilZ domain shown as a red cartoon. The three gating loop positions are shown as cartoons and indicated with their respective colors.

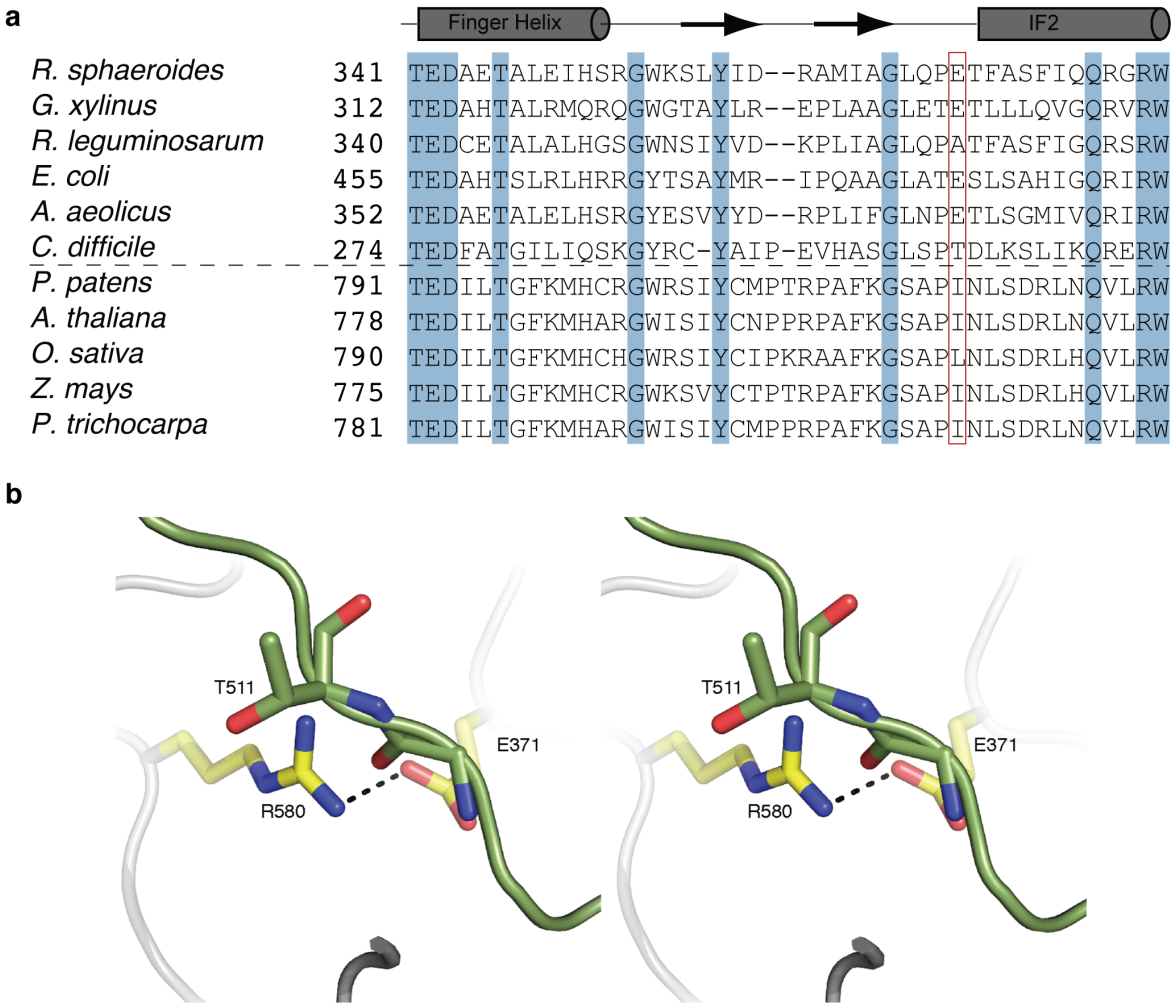

Supplementary Figure 4 A conserved salt bridge stabilizes the resting position of BcsA's gating loop. (**a**) Sequence alignment of pro- and eukaryotic cellulose synthases. In the absence of c-di-GMP, the N-terminal Arg of the PilZ domain's "RxxxR" motif forms a salt bridge with a conserved Glu within the GT domain (framed red). Some outliers, such as BcsA from *R. leguminosarum*, contain an Ala at this position, expected to decrease the dependence on c-di-GMP for cellulose biosynthesis. The *C. difficile* sequence might be shifted in this region and the Asp residue next to the aligned Thr might confer a similar functionality. For eukaryotic cellulose synthases, Ile is the most prevalent residue at the corresponding position. The secondary structure of the aligned sequences is shown as a cartoon based on the *R. sphaeroides* BcsA structure. Pro- and eukaryotic sequences are separated by a dashed line. (**b**) The Glu371-Arg580 salt bridge blocks gating loop insertion in the absence of c-di-GMP. Stereoview of a superposition of pdb 4HG6 and the c-di-GMP/UDP bound structure. Arg580 and Glu371 from 4HG6 are shown as yellow sticks. The inserted state of the gating loop from the c-di-GMP/UDP bound structure is shown in green. A clash between Glu371-Arg580 and the C-terminal end of the gating loop would prevent loop insertion in the absence of c-di-GMP.

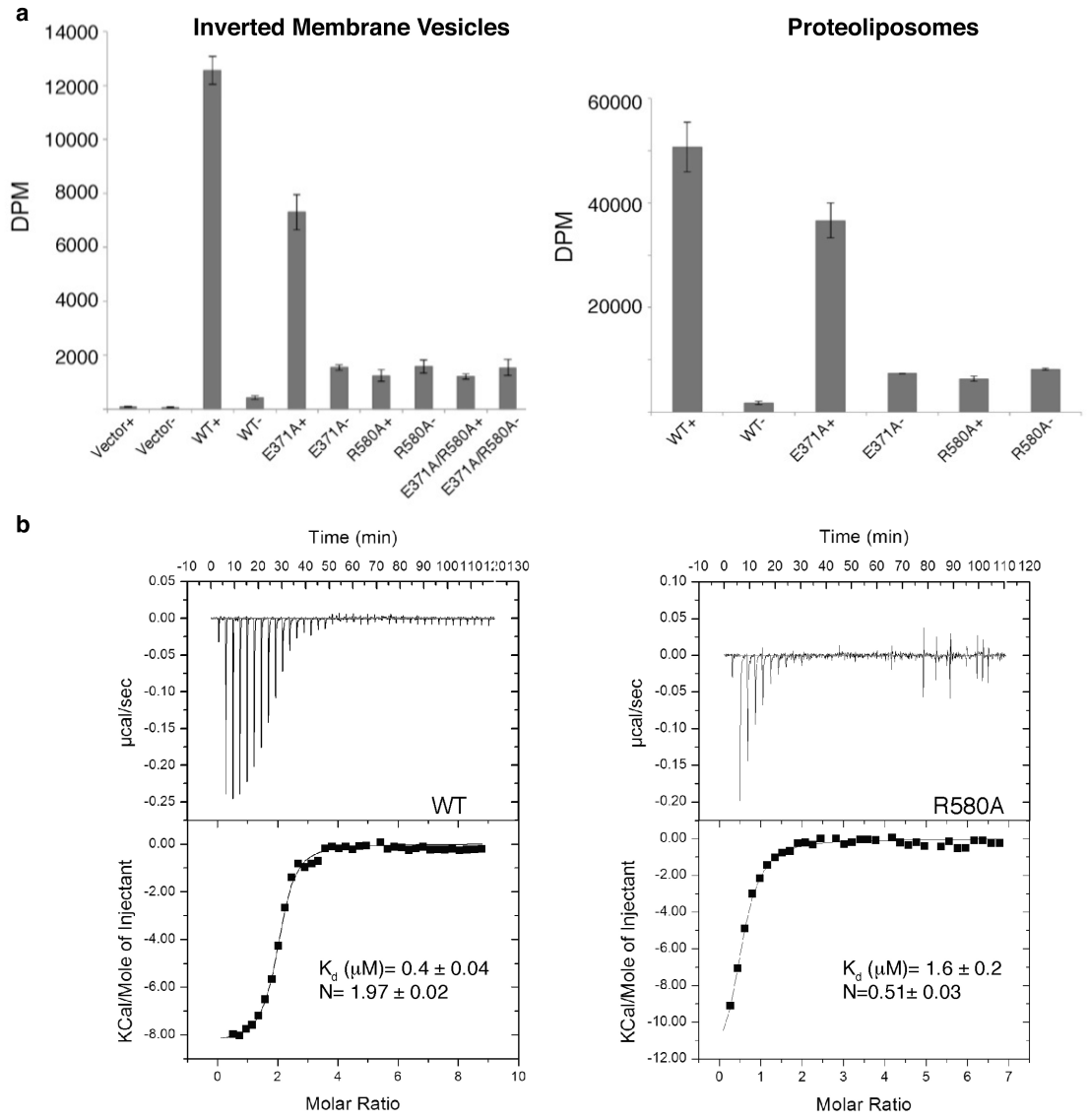

Supplementary Figure 5 Cellulose synthesis activity of BcsA mutants and c-di-GMP binding. (**a**) Cellulose synthesis assays were performed in inverted membrane vesicles and proteoliposomes as described in *the Experimental Procedures*. The amount of ^{3}H-glucose-labeled cellulose produced by each mutant is quantified and graphed. 1 µl of IMV's were used for each mutant. For PL assays, the protein concentrations were matched based on UV absorbance and SDS-PAGE followed by Coomassie staining. The apparent lower activity of the R580A mutant may be due to differences in the relative orientation of the enzyme in the PLs or its overall stability. +/-: Experiments performed in the presence and absence of 30 µM c-di-GMP. All data represent the means ± SD for 3 technical replicates. (**b**) Binding of c-di-GMP to the BcsA-R580A mutant. The ability of the R580A mutant to bind c-di-GMP was assessed using ITC. Left panel, titrating c-di-GMP into wild type (WT) BcsA-B in 1 mM LFCE14 results in an exothermic curve with a K_d of 0.4 µM and a c-di-GMP to BcsA-B stoichiometry of ~2:1 as expected based on the crystal structure. Right panel, BcsA-R580A under the same conditions exhibits a K_d of 1.6 µM and a stoichiometry of ~0.5. The observation that only 1/2-1/4 of the BcsA-R580A population (depending on whether the mutant binds a c-di-GMP monomer or dimer) interacts with c-di-GMP suggests that a fraction of it is structurally compromised, consistent with the results obtained from functional assays (a).

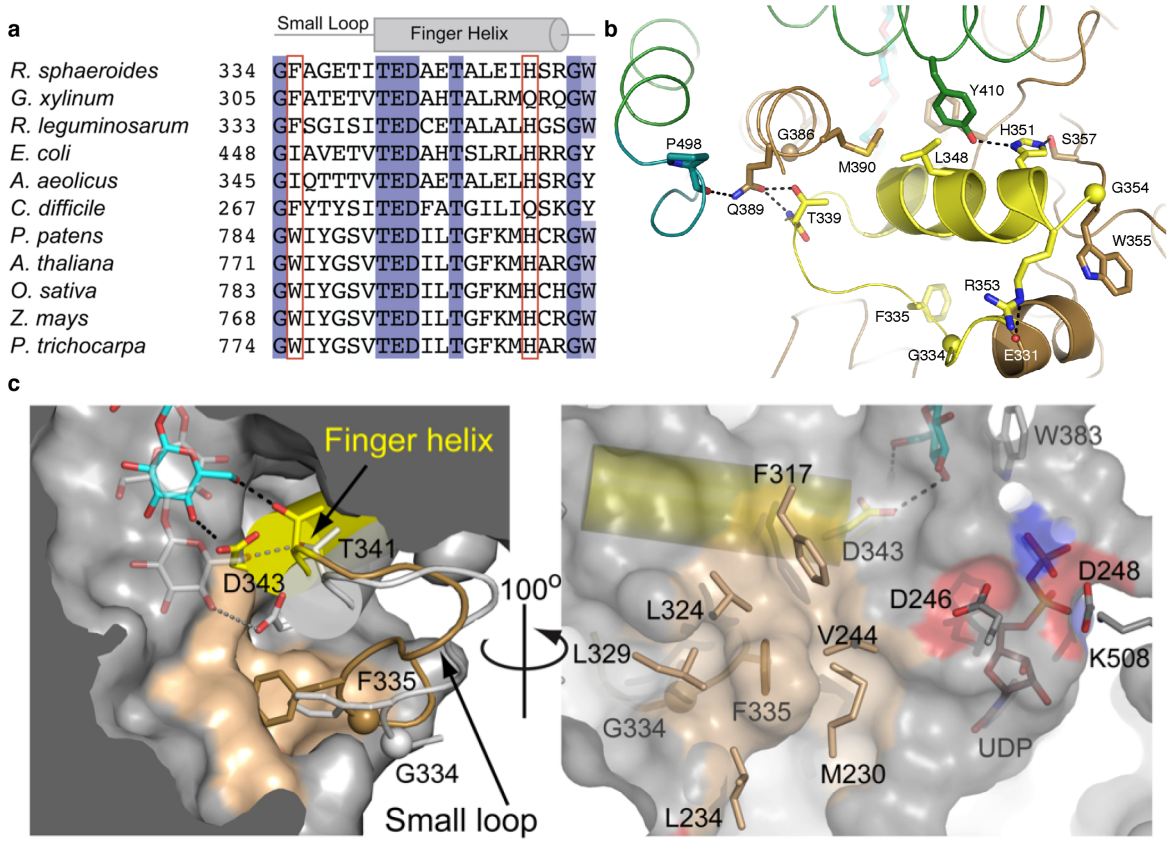

Supplementary Figure 6 The movement of BcsA's finger helix is supported by a small loop. (**a**) Sequence alignment of pro- and eukaryotic cellulose synthases. The small loop contains a conserved Gly residue that is followed by a hydrophobic residue, usually Phe or Trp (framed red). The finger helix carries the invariant "TED" motif at its N terminus and contains a conserved His residue (framed red) followed by a Gly-Trp/Tyr motif that stabilizes the helix at its C terminus. (**b**) The C terminus of BcsA's finger helix (shown as a yellow cartoon) is stabilized by His351, which interacts with the invariant Ser357 and Tyr410. Leu348 packs against Met390 of IF2 and Tyr410 of IF3. Arg353 and Trp355 cap the helix at its C-terminal end. (**c**) Comparison of BcsA's finger helix and small loop in the presence and absence of c-di-GMP. The translocating glucan is shown before and after finger helix movement as gray and cyan sticks, respectively. In the presence of c-di-GMP, Phe335 of the small loop packs into a hydrophobic pocket (shown as a pale orange surface) underneath the finger helix. The preceding conserved Gly334 is shown as a sphere. The position of the finger helix and small loop in the resting state (pdb 4HG6) is shown as a gray cartoon. The right panel shows the same surface boundary as on the left but viewed from the opposite side.

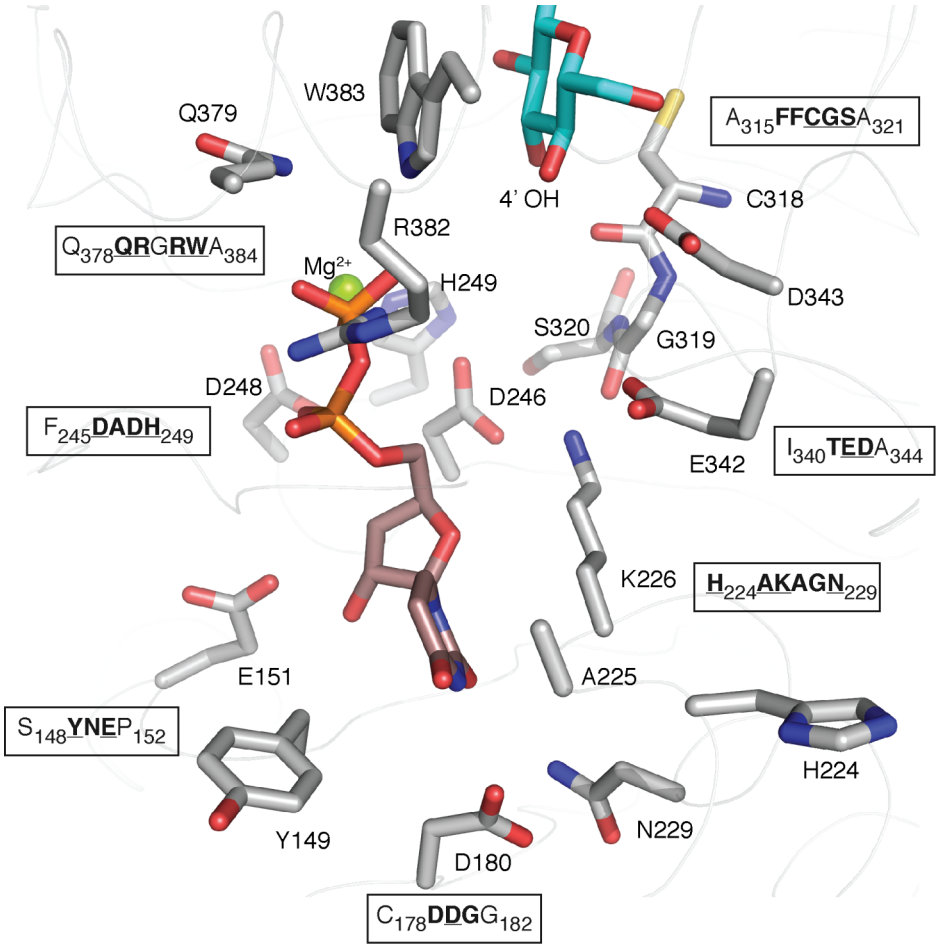

Supplementary Figure 7 Active site signature motifs involved in donor and acceptor coordination. Conserved residues are shown in sticks. The acceptor glucose is stabilized by interactions with Trp383 belonging to the "QxxRW" motif as well as the backbone carbonyl of Cys318 of the "FFCGS" motif. Residues in BcsA's gating loop that also contact UDP (**Fig. 5b**) have been omitted for clarity.